

ARTICLE

Spectral Characteristics of White Organic Light-emitting Diodes Based on Novel Phosphorescent Sensitizer

Xiao-qing Tang, Jun-sheng Yu*, Lu Li, Wen Wen, Ya-dong Jiang

State Key Laboratory of Electronic Thin Films and Integrated Devices, School of Optoelectronic Information, University of Electronic Science and Technology of China, Chengdu 610054, China

(Dated: Received on August 5, 2008; Accepted on September 18, 2008)

White organic light-emitting diodes were fabricated by using a novel phosphorescence bis(1,2-diphenyl-1H-benzoimidazole)iridium(acetylacetonate)[(pbi)₂Ir(acac)] as sensitizer and a fluorescent dye of 4-(dicyanomethylene)-2-*t*-butyl-6-(1,1,7,7-tetramethyljulolidyl-9-enyl)-4H-pyran (DCJTb) codoped into a carbazole polymer of poly(N-vinylcarbazole) (PVK). Through characterizing the UV-Vis absorption spectra, the photoluminescence spectra of (pbi)₂Ir(acac) and DCJTb, and the electroluminescence spectral properties of the WOLEDs, the energy transfer mechanisms of the codoped polymer system were deduced. The results demonstrate that the luminescent spectra with different intensity of (pbi)₂Ir(acac) and DCJTb were co-existent in the EL spectra of the blended system, which is ascribed to an incomplete energy transfer process in the EL process. The efficient Förster and Dexter energy transfer between the host and the guests enabled a strong yellow emission from (pbi)₂Ir(acac) and DCJTb, where (pbi)₂Ir(acac) plays an important role as a phosphorescent sensitizer for DCJTb. With the blue emitting-layer of N,N'-diphenyl-N,N'-bis(1-naphthyl)(1,1'-biphenyl)-4,4'-diamine, the codoped system device achieved white emission. The codoped system showed that its Commissions Internationales de l'Éclairage coordinates were more independent of the variation of bias voltage than those of phosphorescent doped PVK systems.

Key words: White organic light-emitting diode, Phosphorescent sensitizer, Spectrum analysis

I. INTRODUCTION

White organic light-emitting diodes (WOLEDs) have been under active investigation in both academic and industrial fields due to their potential application in back-lights, full-color flat panel displays, and solid state lighting [1-6]. Since the discovery of highly efficient electrophosphorescence, the understanding of the mechanism and optimization of WOLEDs based on them has been of major interest [7-12]. However, phosphorescence in organic molecules is rare at room temperature; the alternative radiative process of fluorescence is common [13-15]. Baldo *et al.* reported the concept of "phosphorescent sensitizer" for improvement of the emission efficiency fluorescent dyes in small-molecule-based organic light-emitting diodes (OLEDs) [16]. It has been demonstrated that the internal efficiency of fluorescence can be as high as 100% by using a phosphorescent sensitizer to excite a fluorescent dye through resonant energy transfer between triplet excitons in the phosphor and singlets in the fluorescent dye [17,18]. Recently, most of WOLEDs based on the phosphorescent sensitizer used the small-molecule as the host. WOLEDs based on a polymer have many manufacturing advantages over small-molecule electroluminescent devices, such as the capability to form thin films using the low-cost techniques of spin-coating technique

or ink-jet printing [19,20]. However, there is little research about phosphorescent sensitizer doped into polymers for white OLEDs so far [21,22].

In this work, using a novel green phosphorescent sensitizer of bis(1,2-diphenyl-1H-benzoimidazole)iridium(acetylacetonate) [(pbi)₂Ir(acac)] and a red fluorescent dye of 4-(dicyanomethylene)-2-*t*-butyl-6-(1,1,7,7-tetra-methyljulolidyl-9-enyl)-4H-pyran (DCJTb) as guest materials, and poly(N-vinylcarbazole) (PVK) as a host, the WOLEDs were fabricated. Herein PVK was chosen as host due to its high energy blue-emissive singlet excited state and the absence of low energy triplet state [23]. By systematically analyzing the photoluminescence (PL) and electroluminescence (EL) spectra of the codoped device at different bias voltages, the energy transfer mechanism from host to guests and spectral characteristics of the devices can be discussed.

II. EXPERIMENTS

The structure of WOLEDs is indium tin oxide (ITO)/PVK:(pbi)₂Ir(acac)(5%):DCJTb(0.2%)/NPB(20 nm)/bathocuproine(BCP)(20 nm)/tris(8-hydroxyquinolate)-aluminum (Alq₃)(10 nm)/Mg:Ag (denoted as device A). In order to compare the difference between the PVK:(pbi)₂Ir(acac):DCJTb dual doping system and PVK:(pbi)₂Ir(acac) single doping system, we also fabricated a device with a structure of ITO/PVK:(pbi)₂Ir(acac) (5%)/NPB (20 nm)/BCP (20 nm)/Alq₃ (10 nm)/Mg:Ag (denoted as device B). The synthesis and characterizations of (pbi)₂Ir(acac) was reported

* Author to whom correspondence should be addressed. E-mail: jsyu@uestc.edu.cn, Tel.: +86-28-83207157

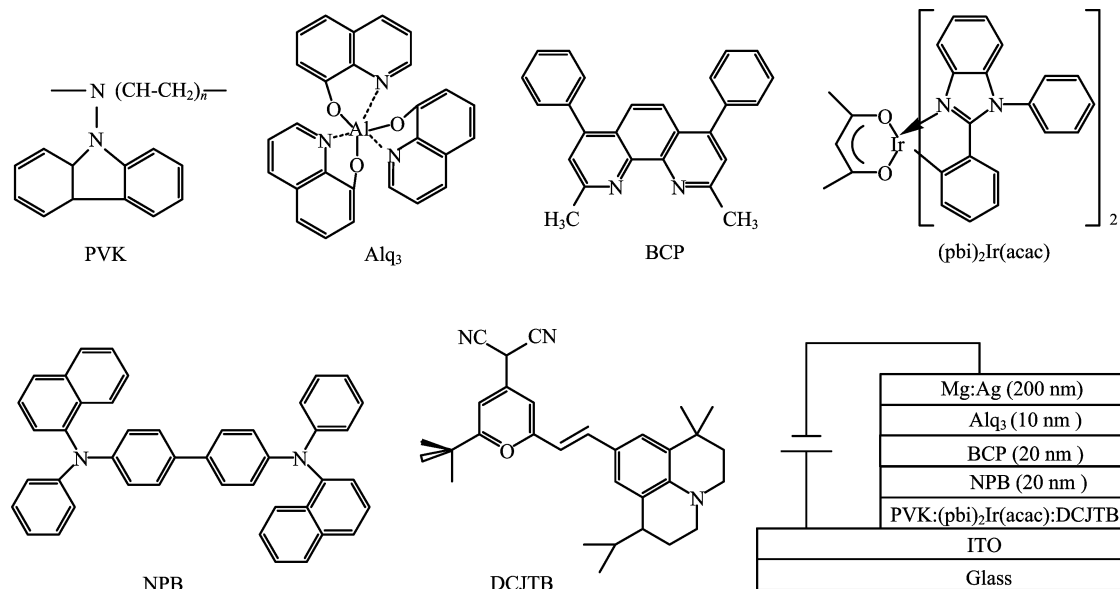


FIG. 1 Molecular structures of organic materials and device architecture.

elsewhere [24]. PVK, DCJTb, NPB, BCP, and Alq₃ were purchased from Sigma-Aldrich Co. and purified by train sublimation twice before use except PVK. The architecture of WOLEDs and molecular structures of the materials used in this work are shown in Fig.1.

ITO-coated substrates with a sheet resistance of $\sim 10 \Omega/\square$ were ultrasonically cleaned with detergent water, deionized water, ethanol, and acetone 10 min each step, and then dried with nitrogen gas. Afterwards, they underwent oxygen plasma treatment for 5 min to enhance the work function of the ITO anode [25]. The emitting layer of co-doped polymer matrix was formed by spin coating from chloroform solution at 4000 r/min for 30 s. NPB, BCP, and Alq₃ films were subsequently deposited at a pressure of 0.01 mPa. The metallic cathode was deposited at a pressure of 0.1 mPa. The deposition rates were 1-2 Å/s for organic materials and 11-13 Å/s for cathode, respectively. The deposition process was *in situ* monitored using a quartz crystal oscillator mounted close to substrate holder. Typical emissive area of the devices was 6 mm \times 6 mm. The EL and PL spectral characteristics of the devices were measured with an OPT-2000 spectrophotometer. Ultraviolet-visible (UV-Vis) absorption was measured with PharmaSpec UV-1700 apparatus (Shimadzu). All the measurements were performed at room temperature in ambient circumstances.

III. RESULTS AND DISCUSSION

The UV-Vis absorption and PL spectra of (pbi)₂Ir(acac) and DCJTb thin film, and PL spectra of PVK host are shown in Fig.2. When measuring the PL spectra, the wavelength of the excited light is 365 nm.

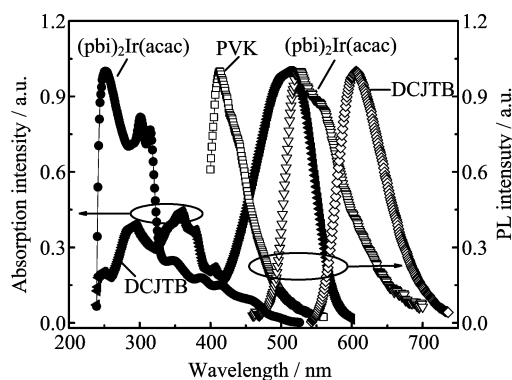


FIG. 2 UV-Vis absorption and PL spectra of (pbi)₂Ir(acac) and DCJTb dopant, and PL spectra of PVK host.

(pbi)₂Ir(acac) phosphor is a kind of benzimidazole derivative, so the absorption peak at ~ 300 nm is part of benzimidazole $\pi \rightarrow \pi^*$ transition in the ligand complex. Metal-ligand charge transfer (MLCT) transition can be observed in the absorption spectra of (pbi)₂Ir(acac) in the long-wavelength region due to the transition from ground state to triplet MLCT excited state [24]. Also there is a good overlap between the PL spectra of PVK and the triplet MLCT absorption of (pbi)₂Ir(acac). Therefore, fast intersystem crossing (ISC) to the triplet state of iridium complex and subsequent emission from this state is built-in feature [23]. Also, we can see that the spectral overlap between the phosphorescent emission band (529 nm) of triplet MLCT states in (pbi)₂Ir(acac) and the absorption band of DCJTb is very large. Therefore, we can predict that there should be efficient energy transfer between PVK host to (pbi)₂Ir(acac) molecules and the (pbi)₂Ir(acac)

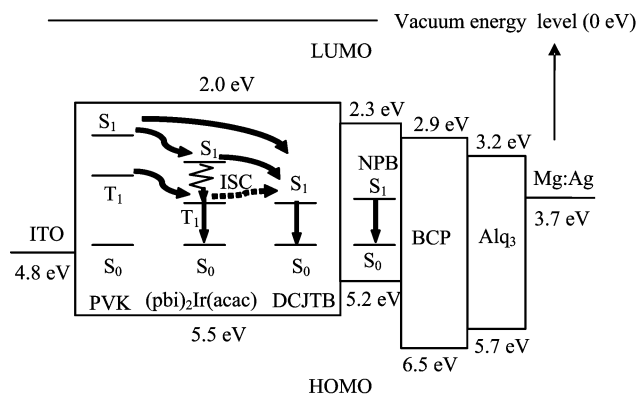
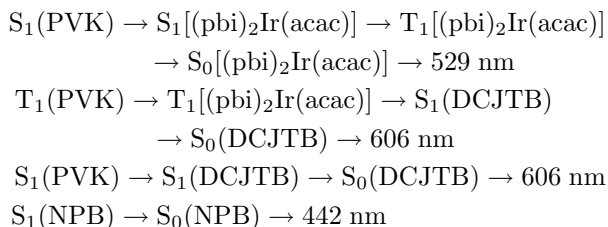


FIG. 3 Schematic energy-level alignment and proposed energy transfer mechanism and light-emission processes in the WOLEDs. The single-excited states (S_1), triplet-excited states (T_1), and single-ground states (S_0).

molecules to DCJTJB accordingly. Furthermore, the small spectral overlap between the fluorescence band of PVK and the absorption band of DCJTJB suggests that the Förster transfer from the single-excited states in PVK to DCJTJB weakly occur.

Figure 3 shows the schematic energy-level alignment of single-excited states (S_1), triplet-excited states (T_1), and single-ground states (S_0) energy diagram and proposed energy transfer mechanism and light-emitting processes in the WOLEDs. It can be inferred that after the injection of electrons and holes from two opposite electrodes, excitons form in the host material of PVK with a ratio of 25% singlet to 75% triplet. Then, the singlet excitons and triplet excitons are transferred to the S_1 and T_1 in $(pbi)_2Ir(acac)$ molecules by a combination of Förster and Dexter processes along with carrier trapping [22]. In $(pbi)_2Ir(acac)$ molecule, the singlet excitons transfer to the triplet states via ISC process. With the presence of red fluorescent DCJTJB dopant, the triplet exciton in $(pbi)_2Ir(acac)$ can transfer to the singlet exciton in DCJTJB through Förster transfer by dipole-dipole coupling. Then, the singlets of DCJTJB decay radiatively and give out of light. With the blue emitting-layer of NPB, the co-doped device can yield white emission. From the above analysis, it can be inferred that the white light-emitting process may be as:



To investigate energy transfer mechanism of this polymer codoped system further, the normalized PL and EL spectra of the devices at a bias voltage of 20 V are shown in Fig.4. Firstly, we can see that there are

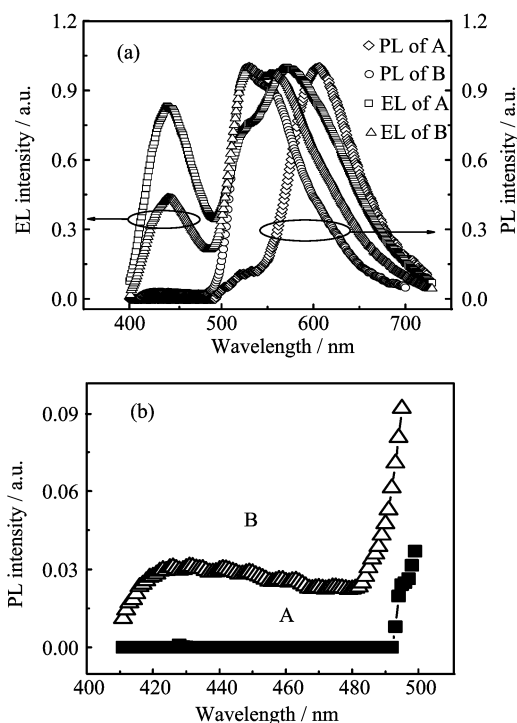


FIG. 4 (a) The PL and EL spectra of devices A and B. (b) The magnification of the PL spectra of devices A and B.

two components in the PL profiles of blends A and B. One is centered at 413 nm ascribed to the light emission of PVK host, and the other is at 529 nm with a shoulder peak at 550 nm corresponding to MLCT triplet emission of $(pbi)_2Ir(acac)$ dopant in PVK: $(pbi)_2Ir(acac)$ blending system. However, compared to the device using phosphorescent sensitizer, which was doped by fluorescent DCJTJB dye, a minor peak at 413 nm originating from PVK host disappears in the PL spectra of device A (Fig.4(b)). There is a minor peak at 529 nm from the MLCT triplet emission of $(pbi)_2Ir(acac)$ molecule, and the other is at 604 nm corresponding to DCJTJB dopant in PVK: $(pbi)_2Ir(acac)$:DCJTJB blending system.

Secondly, in the EL spectra of the devices, there is no PVK emission in the polymer doped system in devices A and B. It can be inferred that energy transfer from PVK to $(pbi)_2Ir(acac)$ is thorough. Device A emits white light with broad EL spectra ranging from 400 nm to 700 nm. In addition, the EL spectra exhibit two primary peaks at 442 and 570 nm and a minor peak at 529 nm. The EL spectra of device B without DCJTJB doping shows two primary emission peaks maxima at 442 and 529 nm. According to the spectral characteristics of these materials discussed above, the minor peak at 529 nm is attributed to the residual phosphorescent emission of $(pbi)_2Ir(acac)$ and the primary peak at 570 nm is due to the phosphor sensitized fluorescent emission of DCJTJB. Here, we can determine that the emission peak at 442 nm comes from NPB. This difference may be explained

as follows: in PLEDs (polymer light-emitting diodes) made of PVK:(pbi)₂Ir(acac), the injected holes and electrons can recombine either on the main chain of PVK to produce blue emission, or then can be trapped by (pbi)₂Ir(acac) with an emission of green light from the triplet of (pbi)₂Ir(acac). In WOLEDs consisting of PVK:(pbi)₂Ir(acac):DCJTB blends, the injected holes and electrons recombine by two processes, i.e., direct energy transfer from main chain PVK to (pbi)₂Ir(acac) or electron and hole directly trapped on (pbi)₂Ir(acac) molecules to produce green emission, and parallel energy transfer from (pbi)₂Ir(acac) phosphorescent sensitizer to DCJTB fluorescent dye for red light emission.

Thirdly, there is a significant difference in the relative emission intensity of the polymer doped devices between PL and EL spectra. As shown in Fig.4, the EL spectra of device A consists of contributions from three emitting centers of NPB, (pbi)₂Ir(acac), and DCJTB, which are quite different from the PL characteristics. The (pbi)₂Ir(acac) contribution has been increased in the EL spectra compared to the PL spectra. The mechanism for exciton formation and emission in the WOLEDs can be deduced from this observation, i.e. exciton formation in PVK, partial PVK-to-dopant energy transfer, and direct exciton formation at the dopant are cooperative in EL as well as in PL process. However, for PL excitation, not only PVK but also the dopants of ((pbi)₂Ir(acac) and DCJTB) can be directly excited at 365 nm as all the components have significant absorption in this wavelength region. On the other hand, comparison of the EL spectra with the corresponding PL spectra reveals that the EL contribution of (pbi)₂Ir(acac) units is larger than that of PL. This is due to the charge-trapping effect of (pbi)₂Ir(acac) in EL process [26].

The emission spectra obtained from devices A and B at different applied voltages from 15 V to 23 V are shown in Fig.5. It can be inferred that the different applied voltages of the codoped devices also affect the spectra of emissive light. In device A, the DCJTB emission peak at 570 nm increases relatively more than NPB emission at 442 nm with the increased bias voltage, and the device achieved a white light at different bias voltages as shown in Fig.6. In contrast, in device B, the NPB emission peak at 442 nm decreases less than the (pbi)₂Ir(acac) emission with the enhanced bias voltage. As a result, the emissive color (shown in Fig.6) changed from yellowish white to yellow emission when bias voltage increased.

According to the Fowler-Nordheim tunneling model [27], the relationship between electric field and the tunneling probability of electrons $Rate_T$ can be expressed as:

$$Rate_T \propto E \exp\left(-\frac{\pi^2}{h} \frac{E_g}{qE} \sqrt{2mE_g}\right) \quad (1)$$

where E is electric field intensity, E_g is bandgap between the highest occupied molecular orbital (HOMO)

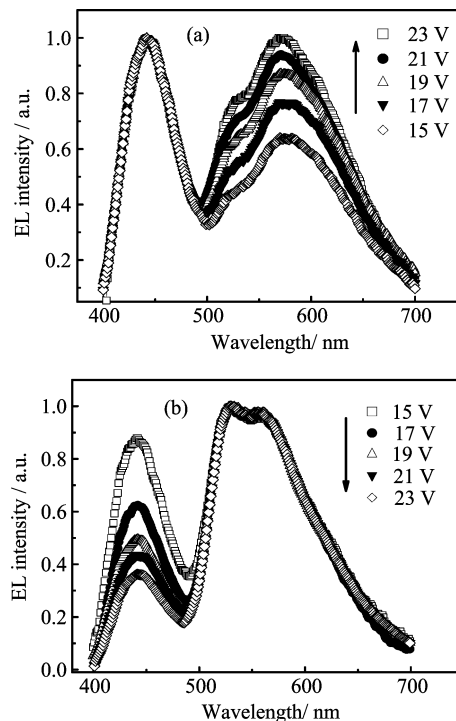


FIG. 5 EL spectra of the device A (a) and B (b) at different bias voltages.

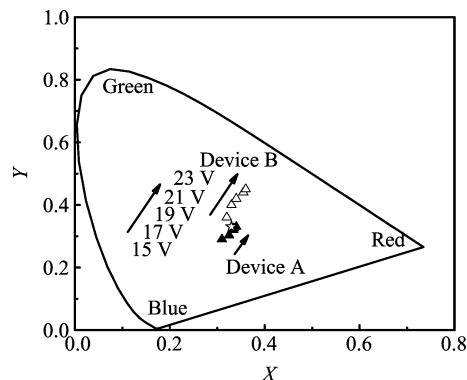


FIG. 6 The CIE (1931) chromaticity diagram with coordinates of devices A and B at various driving voltages from 15 V to 23 V.

and lowest unoccupied molecular orbital (LUMO), m is effective electron mass, and q is electronic charge. As is well known, with the increasing of bias voltage, the electric field intensity of the devices will increase abruptly. From Eq.(1), we can deduce that $Rate_T$ is directly proportional to E . Therefore, this indicates that it is much easier for electrons to tunnel into the codoped system in a high electric field. This leads to more efficient direct exciton formation (carrier recombination) on dopant molecules in EL process due to there being more balance between hole and electron charge carriers with gradually increased bias voltage.

Figure 6 shows the CIE (1931) chromaticity diagram,

with coordinates corresponding to light emission from the polymer doped system devices; data points are shown for both devices A and B biased at different applied voltages. For device B, the CIE coordinates shift from (0.32, 0.36) to (0.36, 0.45), corresponding yellowish white to yellow color. For device A, the CIE coordinates shift from (0.31, 0.29) to (0.34, 0.33), which are very close to the CIE coordinates for pure white light at (0.333, 0.333). The stability of the CIE coordinates as a function of applied voltage of WOLEDs is much higher than those for the case of no fluorescent dye in the polymer doped system device. This provides us an effective way to stabilize the WOLEDs' color purity.

IV. CONCLUSION

In summary, we fabricated phosphorescent WOLEDs using (pbi)₂Ir(acac) phosphorescent sensitizer and a fluorescent dye DCJTb doped PVK system as emitting layer. The characteristics of these copolymer devices indicate that the EL spectra consists of different intensities of (pbi)₂Ir(acac) and DCJTb dopant light emission, and (pbi)₂Ir(acac) acts as not only an acceptor but also a donor in the incomplete energy transfer process between PVK and DCJTb. It also showed that the introduction of a phosphorescent sensitizer of (pbi)₂Ir(acac) can efficiently stabilize the CIE coordinates as well as EL spectra. More importantly, energy transfer in organometallic doped polymeric system is important for material design and device process to achieve high performance phosphorescent WOLEDs. Further investigation of white-emitting polymers based on phosphorescence is still in progress.

V. ACKNOWLEDGMENTS

This work was supported by the National Natural Science Foundation of China (No.60425101), the Program for the New Century Excellent Talents in University of Ministry of Education of China (No.NCET-06-0812), and the Young Talent Project of University of Electronic Science and Technology of China (No.060206).

- [1] T. H. Kim, H. K. Lee, O. O. Park, B. D. Chin, S. H. Lee, and J. K. Kim, *Adv. Funct. Mater.* **16**, 611 (2006).
- [2] C. L. Ho, W. Y. Wong, Z. Q. Gao, C. H. Chen, K. W. Cheah, B. Yao, Z. Xie, Q. Wang, D. Ma, L. Wang, X.

- M. Yu, H. S. Kwok, and Z. Lin, *Adv. Funct. Mater.* **18**, 319 (2008).
- [3] T. S. Shieh, Y. C. Huang, S. T. Yeh, M. T. Chu, and M. R. Tseng, *Int. Soc. Opt. Eng.* **6333**, 633318 (2006).
- [4] H. I. Baek and C. H. Lee, *J. Phys. D: Appl. Phys.* **41**, 105101 (2008).
- [5] J. S. Yu, T. Ma, S. L. Lou, Y. D. Jiang, and Q. Zhang, *Chin. J. Chem. Phys.* **21**, 500 (2008).
- [6] J. Wang, J. S. Yu, L. Li, X. Q. Tang, and Y. D. Jiang, *J. Phys. D: Appl. Phys.* **41**, 045104 (2008).
- [7] Z. S. Su, W. L. Li, B. Chu, M. L. Xu, G. B. Che, D. Wang, L. L. Han, X. Li, D. Y. Zhang, D. F. Bi, and Y. Chen, *J. Phys. D: Appl. Phys.* **41**, 085103 (2008).
- [8] H. You and D. G. Ma, *J. Phys. D: Appl. Phys.* **41**, 155113 (2008).
- [9] L. J. Zhang, Y. L. Hua, X. M. Wu, Y. Wang, and S. G. Yin, *Chin. Phys. B* **17**, 3097 (2008).
- [10] S. Kim, J. Seo, H. K. Jung, J. J. Kim and S. Y. Park, *Adv. Mater.* **17**, 2077 (2005).
- [11] M. A. Baldo, D. F. O'Brien, Y. You, A. Shoustikov, S. Silbey, M. E. Thompson, and S. R. Forrest, *Nature* **395**, 151 (1998).
- [12] Y. Ma, H. Zhang, J. Shen, and C. Che, *Synth. Met.* **94**, 245 (1998).
- [13] J. Wang, J. S. Yu, L. Li, T. Wang, K. Yuan, and Y. D. Jiang, *Appl. Phys. Lett.* **92**, 133308 (2008).
- [14] C. Adachi, M. A. Baldo, M. E. Thompson, and S. R. Forrest, *J. Appl. Phys.* **90**, 5048 (2001).
- [15] S. Kan, X. Liu, J. Zhang, Y. Ma, G. Zhang, Y. Wang, and J. Shen, *Adv. Funct. Mater.* **13**, 603 (2003).
- [16] M. A. Baldo, M. E. Thompson, and S. R. Forrest, *Nature* **403**, 750 (2000).
- [17] G. Cheng, F. Li, Y. Duan, J. Feng, S. Liu, S. Qiu, D. Lin, Y. Ma, and S. T. Lee, *Appl. Phys. Lett.* **82**, 4224 (2003).
- [18] J. Wang, Y. D. Jiang, J. S. Yu, S. L. Lou, and H. Lin, *Appl. Phys. Lett.* **91**, 131105 (2007).
- [19] Z. Chen and D. Ma, *J. Appl. Phys.* **102**, 024510 (2007).
- [20] S. M. King, H. A. Al-Attar, R. J. Evans, A. Congreve, A. Beeby, and A. P. Monkman, *Adv. Funct. Mater.* **16**, 1043 (2006).
- [21] G. He, S. Chang, F. Chen, Y. Li, and Y. Yang, *Appl. Phys. Lett.* **81**, 1509 (2002).
- [22] I. Tanaka, Y. Tabata, and S. Tokito, *J. Appl. Phys.* **99**, 073501 (2006).
- [23] H. Xia, M. Li, D. Lu, C. Zhang, W. Xie, X. Liu, and Y. Ma, *Adv. Funct. Mater.* **17**, 1757 (2007).
- [24] W. Huang, J. T. Lin, C. Chien, Y. Tao, S. Sun, and Y. Wen, *Chem. Mater.* **16**, 2480 (2004).
- [25] J. S. Yu, W. Z. Li, Y. D. Jiang, and L. Li, *Jpn. J. Appl. Phys.* **46**, L31 (2007).
- [26] X. Q. Tang, J. S. Yu, L. Li, J. Wang, and Y. D. Jiang, *Acta. Phys. Chim. Sin.* **24**, 1012 (2008).
- [27] R. H. Fowler and L. W. Nordheim, *Proc. Roy. Soc. (London)* **A119**, 173 (1928).